The College of Engineering
University of Wisconsin–Madison

Wisconsin Electric Machines and Power Electronics Consortium

RESEARCH REPORT
93-32

Quasi Current Resonant DC Link AC/AC Converter

H. Nakamura and Y. Murai
Dept. of Electronics and Computer Engineering
Gifu University
1-1 yangido, Gifu, Gifu 501-11
Japan

Thomas A. Lipo
Dept. of Electrical and Computer Engineering
University of Wisconsin-Madison
1415 Johnson Drive
Madison, WI 53706

WEMPEC

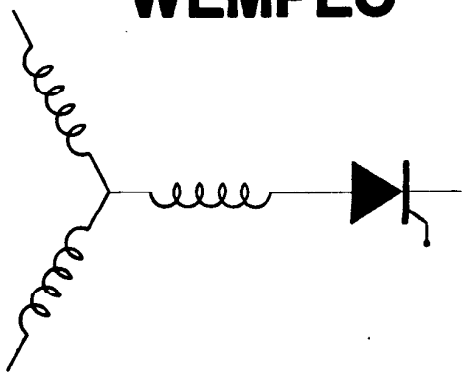

Department of Electrical and Computer Engineering
1415 Johnson Drive
Madison, Wisconsin 53706

Quasi Current Resonant DC Link AC/AC Converter

H. Nakamura Y. Murai

Dept. of Electronics & Computer Eng.
Gifu University
1-1 yanagido, Gifu, Gifu 501-11
Japan.

T. A. Lipo

Dept. of Electrical & Computer Eng.
University of Wisconsin-Madison
1415 Johnson Drive
Madison, WI 53706, U.S.A.

Abstract - A new quasi current resonant dc link (QCRDCL) topology has been developed in this paper. Although prototype current resonant dc link topologies for AC/AC power conversion has had such problems as irregular high current peaks, uncontrollable pulse width, etc., this new topology enables the AC/AC conversion system to have the properties wherein the current peak is limited and the pulse width is adjustable. The system begins to assume an adjustable-width flat-topped current shape, whereby the system becomes particularly suitable for high power application. With control of the pulse width a very fine load current regulation can be obtained. In this system, an open loop PWM control has been adopted and almost the same quality of output waveforms as the conventional current source inverter has been achieved.

I. INTRODUCTION

In recent years, many types of resonant power conversion topologies have been developed for ac motor drives [1]-[5]. The basic configurations of these topologies are of the conventional VSI or CSI inverters with an additional capacitor and inductor for the resonant tank. Although such circuits can reduce the high frequency switching losses to a minimal value by means of zero-voltage or zero-current switching, they have a particular problem in that the resonant pulse peak is much higher than source voltage or current, so that the system needs much higher voltage or current rating of the switching devices than conventional hard switched inverters. Furthermore, the output waveform control is solely carried out by PDM (pulse density modulation) because of lack of pulsewidth adjustments. Hence they need extremely high frequency switching to achieve high quality output waveform control.

In order to solve these problems, the actively clamped resonant dc link inverter [2] and other sophisticated circuits which limit the link voltage have been presented for use with voltage resonant converters [4],[5]. In case of current resonant converters, the authors have proposed a current peak limiting circuit for a series resonant dc link converter using a saturable core in 1991 [3]. The clamping action in this case was realized by utilizing a saturable core for a resonant inductor without using any additional active elements. Although this converter works very well with a pulse-split control principle and has some degree of current adjustment, it could not, however, easily produce wider flat-topped current waveforms.

This paper presents a new converter concept having a highly adjustable flat-topped current pulse. The system operates with partially resonant or quasi-resonant topology and the pulse peak is always maintained at the dc link current value. Thus, the irregular current peak stress of the previous basic circuit is reduced and the current rating of the devices is remarkably reduced. Owing to the ability of the circuit to produce a variable current pulse width with constant pulse amplitude, open loop PWM control can be adopted and nearly the same output performance as the conventional current source GTO inverters can be achieved. In the proposed system all of the switches are naturally commutated thyristors with no snubbers. Hence, the circuit is low cost concept, with great potential in high power applications.

II. PRINCIPLES

Figure 1 shows the overall configuration of the basic series resonant dc link converter. The capacitance C_0 and inductance L_0 form high frequency resonant circuit and both the three capacitors at input and output are used as filters to bypass high frequency components to maintain the resonant frequency. The inductance L_d is to superimpose a dc current onto the high frequency resonant currents to allow for unidirectional switches in the converters (i.e. thyristors). Figure 2 shows the proposed quasi resonant converter with additional three thyristors (T_{ha}, T_{hb} and T_{hc}). These thyristors are used to control the resonance of prototype current pulses.

To explain the converter operation, the switching condition and operational waveforms are shown in Fig. 3 with a modified single phase equivalent circuit. For the equivalent circuit, the following assumptions are made. As the input and output filter capacitors are very large compared to the resonant capacitor C_0, these elements are represented as a voltage source V_s. Since the inductance L_d is large enough to work as a current source, the resonant frequency is decided by C_0 and L_0. A thyristor T_h represents the four thyristors conducting in series noted in black in Fig. 2. During starting of converter operation, the thyristors T_{hb} and T_{hc} are kept on, while T_{ha} remains off. The system operates as a prototype series resonant converter as shown in Fig. 1 and the operating waveform is shown in Fig. 3(a). After establishing a dc current I_d (= steady state value of i_d; almost constant), quasi resonant operation begins to take place as shown in Fig. 3(b).

These processes can be described as follows according to each mode.

A. Series resonant operation

The operation of converter divided into three modes. Waveform of i_d is depicted by the dotted line in the same area of i_s. The periods while thyristors conduct are drawn in oblique lines in the lower part of Fig. 3 (a). The first and second pulses express the starting condition and the third one expresses the beginning of steady state operation.

(a) Mode 0 ($0< t < t_{01}$) : Initially, C_0 is discharged and no current flows in L_d. The prototype series resonant operation is utilized by triggering thyristors T_h and T_{hc}. The resonant current i_s flows sinusoidally and i_d increases linearly.

(b) Mode 1 ($t_{01}< t < t_{02}$) : When current i_s reaches zero, thyristor T_h turns off. Subsequently T_{hb} is turned on so that the current i_d flows through T_{hb} and charges C_0 up to the polarity as shown in the figure (mode 1). The resonant capacitor voltage V_{C0} increases linearly. When resonance occurs, the voltage V_s is obtained as follows:

$$V_s = V_d - V_{C_a} - V_{C_L} \qquad (1)$$

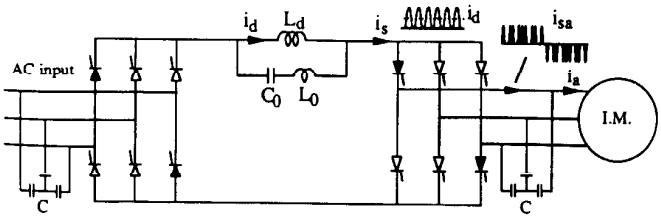

Fig. 1. Basic series resonant dc link converter.

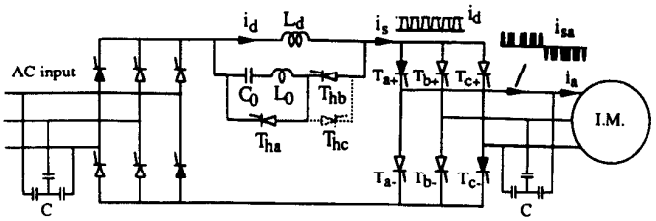

Fig. 2. Proposed quasi resonant dc link converter.

0-7803-1243-0/93$03.00 © 1993 IEEE

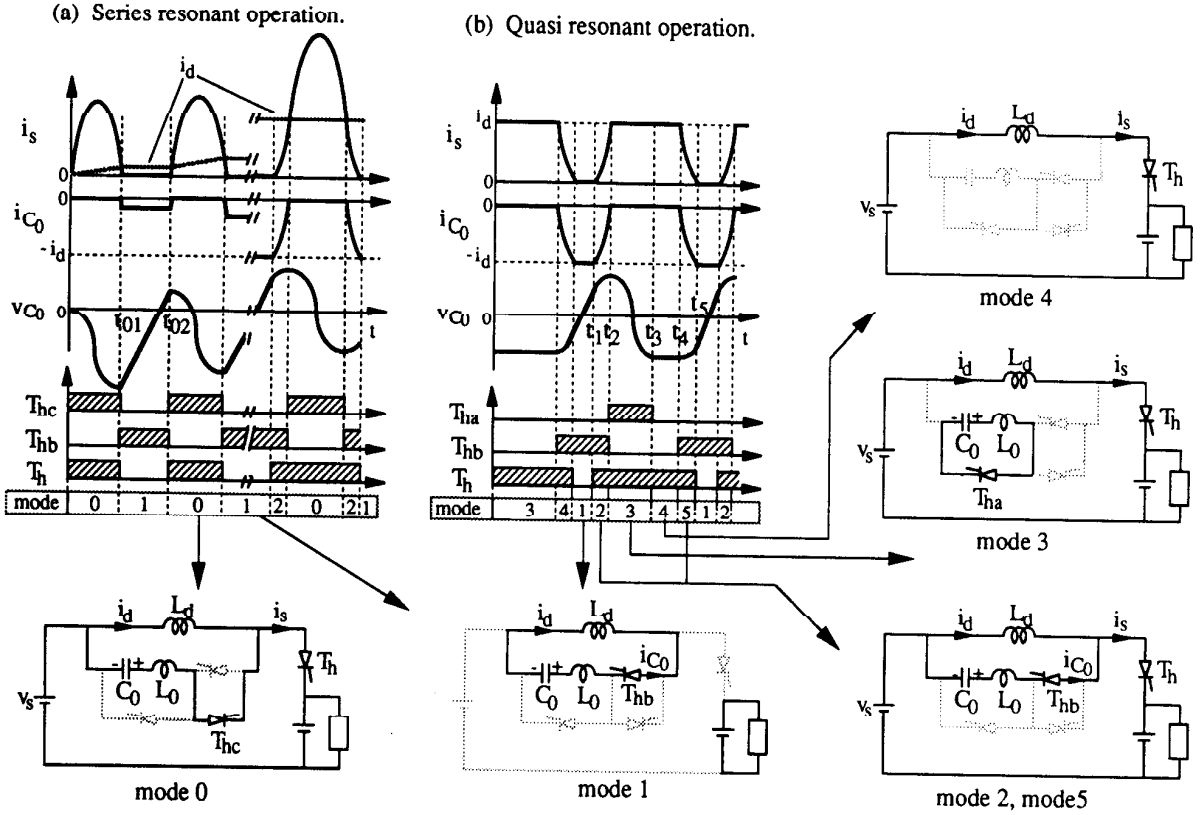

Fig. 3. Modefied single phase equivalent circuit and operating waveforms.

When V_S reaches a certain threshold value, mode 0 operation is reinitiated. As i_{C0} has a negative polarity at this instant, mode 2 is entered between mode 1 and mode 0 until i_{C0} reaches zero.

B. Quasi resonant operation

After the series resonant operation imposed during starting, quasi resonant operation is ready to begin. When the quasi resonant starts after mode 1, five modes appear during normal operation.

(a) Mode 2 ($t_1 < t < t_2$) : If V_S reaches the threshold value in the mode1, T_h is triggered at the beginning of mode 2. During mode 2, i_{C0} increases up to zero and i_S increases up to I_d.

(b) Mode 3 ($t_2 < t < t_3$) : When i_S equals to I_d, i_{C0} becomes zero and thyristor T_{hb} turns off. At the same time, upon triggering T_{ha}, resonance occurs through C_0 and L_0, and the charge of C_0 changes to the inverse polarity. The resonant current flowing through T_{ha} reaches zero and T_{ha} turns off.

(c) Mode 4 ($t_3 < t < t_4$) : C_0 and L_0 are separated from L_d and the current i_S flows through L_d. By varying the duration time of mode 4, an optimal current can now be supplied to the load.

(d) Mode 5 ($t_4 < t < t_5$) : When T_{hb} is triggered again, i_S decreases to zero as i_{C0} flows into C_0. If i_S becomes zero, thyristor T_h is turned off and one resonant process is completed.

A modified quasi-resonant dc link circuit is shown in Fig. 4 which is usable for the quasi-resonant operation. A minimum pulse width can again be generated since there is no need for a reversing time in mode 3 owing to the thyristor bridge. A detailed analysis of this circuit operation is presented in the Appendix.

III. COMPARISONS BETWEEN QCRDCL AND BASIC CRDCL

The resonant current pulse waveforms of QCRDCL and that of basic current resonant dc link (CRDCL) converter are illustrated in Fig. 5(a) and (b), respectively. Both of the average values of current pulses are equal and the duration times of the dead zone between two adjacent pulses are kept equal. As shown in Fig. 5(a), the pulse peak is as high as at least two times of the average current I_d. On the other hand, in Fig. 5(b), the current pulse shape is flat-topped and the pulse width is variable, the limited peak value I_d is much lower

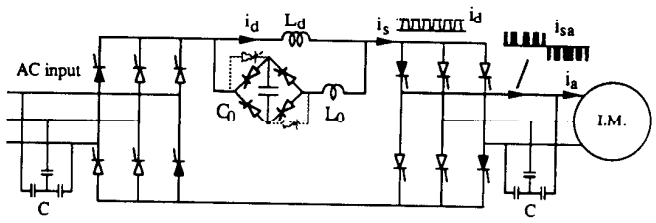

Fig. 4. Modefied quasi resonant dc link converter.

than the peak in Fig. 5(a). Also, the rms current becomes lower. Hence, it is clear that the QCRDCL can transfer higher power with low rated switches than with the basic prototype converter.

To establish the peak and rms current value, simulated results are shown in Fig. 6. The basic prototype converter operates with a 20 kHz switching frequency and the QCRDCL operates at the switching frequency varying from 2 kHz to 20 kHz. Both average output currents and the initial voltages of C_0 at the beginning of the resonance are maintained at the same values of 5A and 80V respectively. The dead zones are adjusted to have a constant value of 30 μs by changing C_0 of the QCRDCL. In the case of the prototype converter, C_0 = 0.9 μF and L_0 = 33 μH. The peak current of prototype converter was 18.8 A and the rms current was 8.6 A.

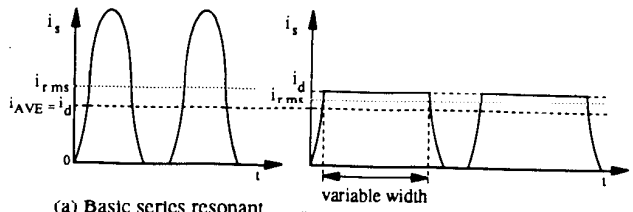

(a) Basic series resonant waveform.
(b) Quasi current resonant waveform.

Fig. 5. Example of current pulse waveforms.

peak value	18.85 (A)
rms	8.60 (A)

The basic converter.

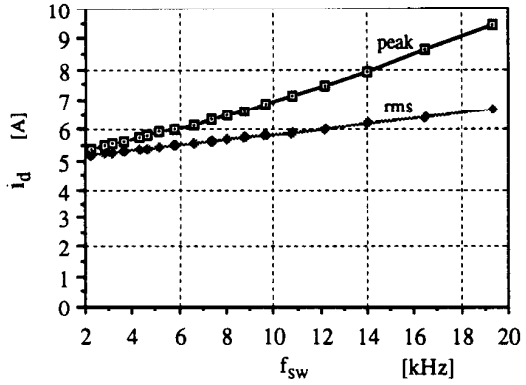

Fig. 6. Peak and rms current of the QCRDCL converter.

Comparing to these values, for instance, the peak current and the rms current of QCRDCL were 9.4 A and 6.6 A respectively for a switching frequency of 20 kHz. If the switching frequency decreases to 2 kHz, the peak current and the rms current become 5.4 A and 5.2 A, respectively. Accordingly, the peak and rms current clearly decreases under the same average current as the switching frequency becomes lower.

The relationships between the resonant capacitor voltage and I_d are illustrated in Fig. 7. When the link current i_s rises from zero to I_d and subsequently falls in the quasi-resonant mode, the energy stored in C_0 is used. To ensure that I_d becomes zero, sufficient voltage must be impressed on v_{C0}. The necessary voltage for v_{C0} is calculated from equation (8) in the Appendix. The required value is proportional to I_d and becomes smaller as the characteristic impedance Z_0 increases. Since I_d decreases as the switching frequency becomes lower in Fig. 6, if the QCRDCL is operated by lowering the frequency switching, the necessary peak voltage of v_{C0} becomes lower as well.

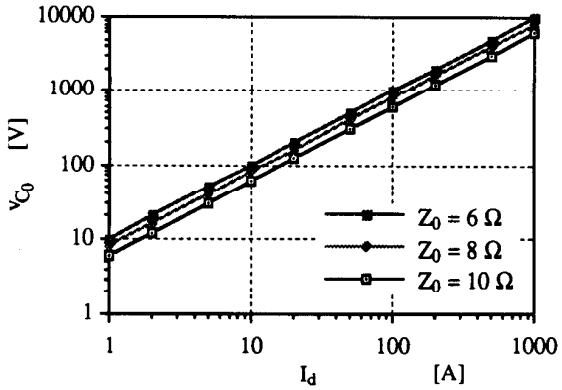

Fig. 7. Necessary voltage of v_{C_0} to make I_d into zero.

IV. PWM CONTROL METHOD

Although various kinds of PWM methods are applicable to QCRDCL, a simple method was adopted to investigate the performance of QCRDCL. Fortunately, since QCRDCL has the ability of variable pulse width, the PWM control method was adopted for the control of the output waveform. Using the PWM control method, accurate control of the output waveform is possible with a low switching frequency.

The reference control waveforms used in the PWM algorithm are shown in Fig. 8. These waveforms have been chosen to reduce the switching frequency. The PWM pulse pattern is determined by

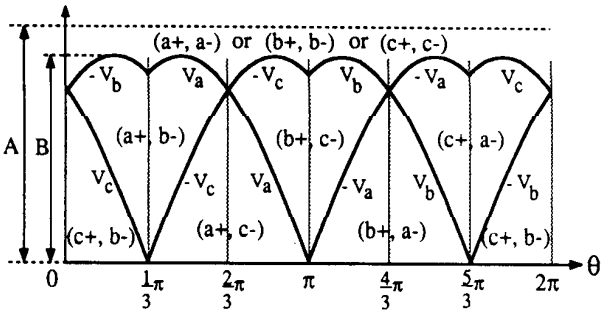

Fig. 8. Reference control waveforms used in the PWM algorithm.

comparing the reference waveforms and triangular carrier waveforms. The triangular waveform is scanned within the reference waveform, and commutated switches are selected as noted (e.g. a+,c-) corresponding to the each area shown in Fig. 8. That is, two thyristors T_{a+} and T_{c-} are triggered when the resonant current flows to the output. During the interval when the carrier waveform is scanned to be above the area of reference waveform, the output is shorted. Both sides of one arm of the output thyristor bridge are triggered, for example (a+,a-), (b+,b-) or (c+,c-). The modulation index B/A is the factor that changes amplitude ratio of reference waveforms to carrier waveform. It is used to adjust the magnitude of the reference waveform according to the dead time between resonant pulses.

When the QCRDCL is controlled by a PWM control, its operation is a bit different from that of a CSI inverter. To explain this difference, PWM reference waveforms and simulated resonant current waveforms of the QCRDCL are shown in Figs. 9 (a) and (b). These traces show the line current of the output three phases. The carrier frequency is assumed to be 2 kHz. The reference waveforms are such that i_a^* continues to flow and i_b^* and i_c^* flow alternately during one cycle of the carrier waveform. As shown by the simulated waveforms the conducting phases can not be changed while a current pulse flows. If a change of phase selection occurs in the reference waveforms, quasi-resonance must be made to terminate and the next pulse directed into different phases. Therefore, i_a of the QCRDCL is separated into three parts during one cycle of the carrier waveform. When the output phases change, a dead time exists and current does not flow into the output phases. This condition can be regarded as equivalent to a short condition of the current resonant link. There are four portions of the dead zone during one cycle of the carrier waveform. When the shorted mode is taking place, a compensated short circuit mode time (the duration time for which the short condition is effective) is used. This compensated value is obtained by subtracting the sum of the dead time between the resonant pulses from the shorted mode time of the reference waveforms. The duration time of A minus B shown in Fig. 8 requires more than the sum of the dead time. In this simulation, the modulating index was 0.7.

In Fig. 9(b), it can be noted that an oscillation is superimposed on the resonant current. Because the dc inductance L_d has a finite value, by changing the input and output voltage, I_d is altered according to the voltage applied to L_d. As the output voltage is controlled in open loop fashion, the fluctuation of I_d affects the output control. But the oscillating current band width is limited to a sufficiently narrow value compared to I_d so that the ripple in the link current does not materially affect the harmonic content in the output current waveform. It should be mentioned at this point that a similar effect is caused in CSI inverter drives as well by the necessity of a finite link inductance without serious consequences. However, in order to substantially improve the accuracy of the output control, feedback control will clearly be indispensable.

V. RESULTING WAVEFORMS

A. Simulation waveform

Figure 10 shows the results obtained by computer simulation of the three phase circuit in Fig. 2. The waveform at the chief spot of the circuit are exhibited. The traces show one of three output

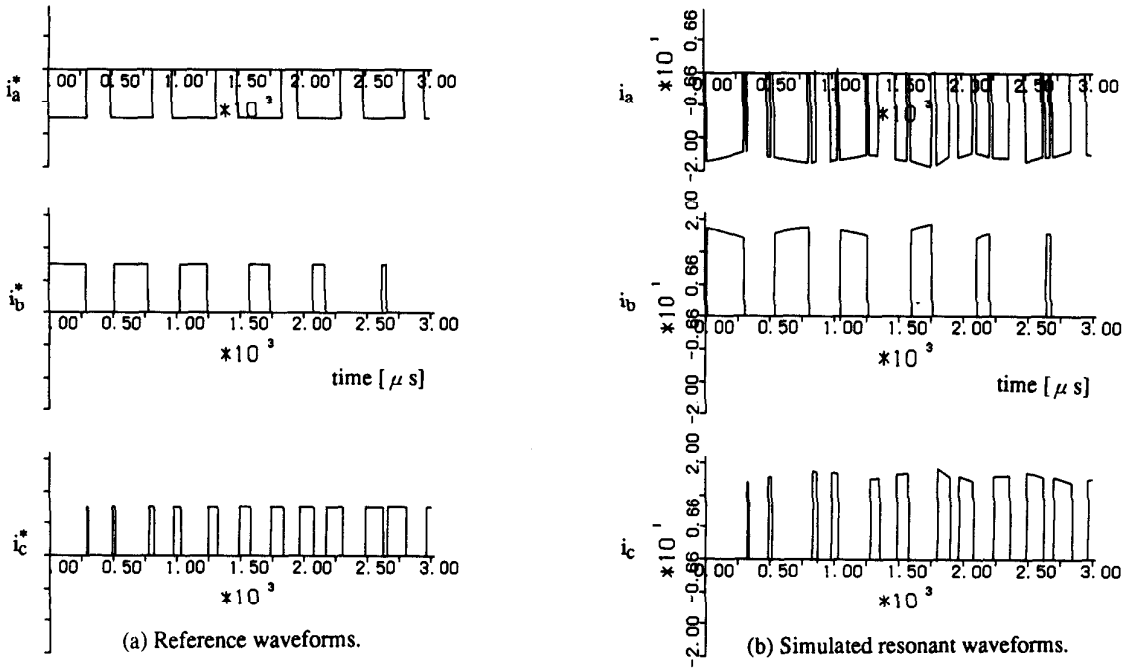

Fig. 9. PWM control reference waveform and resonant current waveforms flow into output three phases.

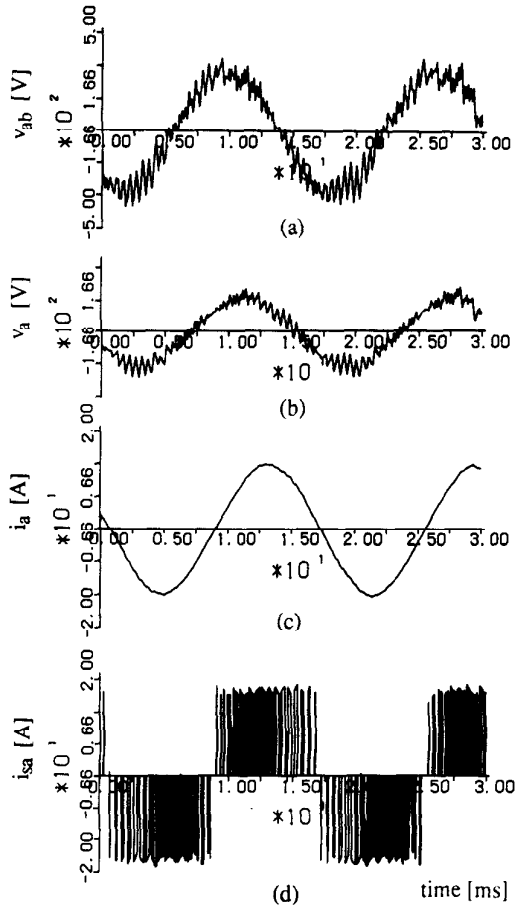

voltages and the currents; v_{ab}, v_a, i_a and i_{sa} are shown in Fig. 10 (a), (b), (c) and (d) respectively. Fig. 10 (e) and (f) show i_d and the short mode current in the output. The load is assumed to be a symmetrical three phase circuit with a series R - L for each phase. The load parameters are R = 10 Ω, L = 250 mH, output frequency of 60 Hz, and a load voltage of 200 V. The source voltages are also balanced three phase at 200 V. The circuit parameters are L_0 = 50 μH, C_0 = 0.5 μF, L_d = 40 mH, C_L = 20 μF and the carrier frequency = 2 kHz. It is apparent that smooth sinusoidal output waveforms can be obtained from this circuit concept.

B. Experimental waveform

To confirm the operating principle of the QCRDCL, experiment by means of a single phase circuit configuration has also been performed. Figure 11 shows waveforms of the resonant current i_s and the resonant capacitor voltage v_{C0}. The conditions are such that V_d = 80 V and load resistance is 20 Ω. The over-shoot during the rising and falling of i_s are caused because thyristors can not block the

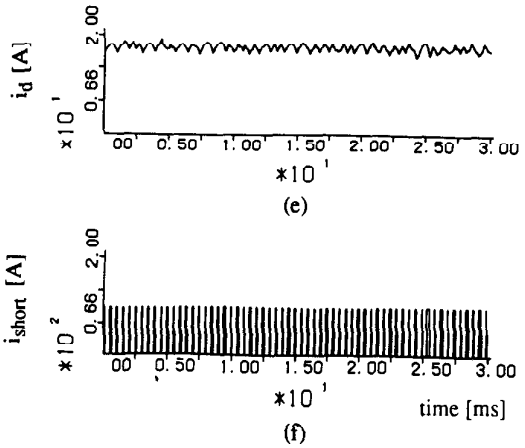

Fig. 10. Simulated output waveforms.

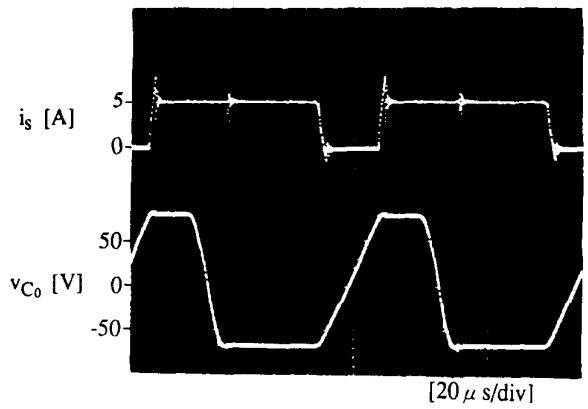

Fig. 11. Experimental waveforms.

resonant current in this brief moment due to discharge of the storage charge when thyristor makes its reverse recovery. The flat area of v_{C0} after i_S reaches I_d is needed to ensure sufficient turn off time of thyristor T_{hb}.

VI. CONCLUSION

In this paper, a new quasi resonant current type dc link converter (QCRDCL) was proposed. The features of this new converter are that the generated pulse waveforms are flat-topped and that the pulse width is adjustable. By means of accurate adjustability of pulse width, open loop PWM control was adopted without using any voltage feed back.

The resulting output waveforms are as good as the same quality of conventional CSI inverter. The QCRDCL can also control output accurately with low frequency switching and is very suitable for high power conversion. Since the switching is done by soft switching, the QCRDCL can realize low switching losses with low EMI.

In this paper, an open loop PWM control was adopted to simplify the control and to evaluate the fundamental capability of the QCRDCL. In order to improve the output control under a wide range of load conditions advanced controls are under investigation.

REFERENCES

[1] Y. Murai, T. A. Lipo: "High Frequency Series Resonant DC Link Power Conversion," IEEE IAS Annual Meeting Conf. Rec., pp. 772-779, 1988.

[2] D. M. Divan, G. Skibinski: "Zero-Switching-Loss Inverters for High-Power Applications," IEEE Trans. Ind. Applic., IA-25, pp. 634-643, 1989.

[3] Y. Murai, H. Nakamura, T. A. Lipo, M. T. Aydemir, "Pulse - Split Concept in Series Resonant DC Link Power Conversion for Induction Motor Drives," IEEE IAS Annual Meeting Conf. Rec., pp. 776-781, 1991.

[4] J. He and N. Mohan, "Parallel Resonant DC Link Circuit - A Novel Zero Switching Loss Topology with Minimum Voltage Stresses," IEEE Trans. Power Electronics, vol. 6, no. 4, pp. 687-694, Oct. 1991.

[5] J. G. Cho, H. S. Kim and G. H. Cho, "Novel Soft Switching PWM Converter Using A New Parallel Resonant DC - Link," IEEE PESC Conf. Rec., pp. 241-247, 1991.

[6] M. Hombu, S. Ueda, A. Ueda, "A Current Source GTO Inverter with Sinusoidal Input and Outputs," IEEE Trans. Ind. Applic., vol. IA-23, no. 2, pp. 247-255, 1987.

[7] S. Nonaka, Y. Neba, "New GTO Current Source Inverter with Pulsewidth Modulation Control Techniques," IEEE Trans. Ind. Applic. vol. IA-22, no. 4, pp. 666-672, 1986.

[8] G. Joos, G. Moschopoulos, P. D. Ziogas, "A High Performance Current Source Inverter," IEEE PESC Conf. Rec., pp. 123-130, 1991.

APPENDIX

Analysis of Circuit Operation

To analyze fundamental operation of the QCRDCL, a single phase equivalent circuit can be utilized. It is assumed that all of the devices and components are ideal. During the initial start-up condition, current I_d flows into L_d and voltage v_{C0} is applied to C_0. The moment that T_h is triggered, the voltage which emerges across T_h is

$$V_s = V_d - V_{C_0} - V_{C_L}. \tag{1}$$

and the circuit equations become

$$E = L_d \frac{di_d}{dt} + V_s$$
$$L_d \frac{di_d}{dt} = \frac{1}{C_0} \int i_0 \, dt + L_0 \frac{di_0}{dt} \tag{2}$$

The resulting current i_S during mode 2 is obtained as follows:

$$i_s(t) = \frac{V_s}{Z_0} \sin\omega_0 t + I_d (1 - \cos\omega_0 t) \tag{3}$$

$$v_{C_0}(t) = v_{C_0(t=t_1)} - V_s \cos \omega_0 t - I_d \sin \omega_0 t \tag{4}$$

where

$$\omega_0 = \frac{1}{\sqrt{L_0 C_0}} \tag{5}$$

$$Z_0 = \sqrt{\frac{L_0}{C_0}}. \tag{6}$$

The duration time of mode 2, or the time interval $[t_2-t_1]$, is

$$t_2 - t_1 = \frac{1}{\omega_0} \tan^{-1} \frac{I_d Z_0}{V_s}. \tag{7}$$

and the value of v_{C0} at time t_2 is

$$v_{C_0}(t_2) = v_{C_0(t=t_1)} - \sqrt{V_s^2 + I_d^2 Z_0^2}. \tag{8}$$

This becomes the maximum value of v_{C0}.

During mode 3, or the time interval $[t_3-t_2]$, the equations of the circuit are obtained as follows:

$$i_s(t) = \frac{V_s}{Z_0} \sin\omega_0 t \tag{9}$$

$$v_{C_0}(t) = v_{C_0(t=t_2)} - V_s \cos \omega_0 t \tag{10}$$

The time interval $[t_3-t_2]$ is

$$t_3 - t_2 = \pi \sqrt{L_0 C_0}. \tag{11}$$

During mode 4, current i_S flows through L_d so that $i_s = I_d$. During the mode 5, the equations for i_S and v_{C0} are described as follows:

$$i_s(t) = \frac{V_s}{Z_0} \sin\omega_0 t + I_d \tag{12}$$

$$v_{C_0}(t) = v_{C_0(t=t_4)} - V_s \cos \omega_0 t \tag{13}$$

The time interval $[t_5-t_4]$ is

$$t_5 - t_4 = \frac{1}{\omega_0} \sin^{-1} \left(- \frac{I_d Z_0}{v_{s(t=t_4)}} \right). \tag{14}$$

During mode 1, v_{C0} is charged by i_d up to the required voltage to generate the next resonant pulse. Assuming that i_d is almost constant, the equations are obtained as follows:

$$i_s(t) = 0 \tag{15}$$

$$v_{C_0}(t) = v_{C_0(t=t_5)} - \frac{I_d}{C_0} t \tag{16}$$

The time interval $[t_6\text{-}t_5]$ is

$$t_6 - t_5 = \frac{C_0}{I_d}\left(v_{C_0(t=t_6)} - v_{C_0(t=t_5)}\right) \tag{17}$$